

# INFLUENCE OF HEEL ON YACHT SAILPLAN PERFORMANCE

**Fabio Fossati**, Full Professor, Wind Tunnel - Politecnico di Milano, Italy, fabio.fossati@polimi.it  
**Sara Muggiasca**, Researcher, Department of Mechanical Engineering, Politecnico di Milano, Italy

## SUMMARY

This paper presents research activities carried out by the authors to investigate the influence of heel on yacht sailplan performance by means of wind tunnel test techniques and CFD numerical simulations. Main results concerning wind tunnel testing activities carried out in the Politecnico di Milano Twisted Flow Wind Tunnel investigating the upwind performance of sails both heeled and upright are presented. Finally the heeled plane approach which is largely used in the aerodynamic models available up to-date for VPP use is outlined and discussed

## 1. INTRODUCTION

Sailing yacht heeling effect on sails aerodynamics represents one of the tougher issue of upwind aerodynamics ([1] [3] [6] [7]) and some discussions have been recently found in literature [8]. In fact this is a very complex topic with strong implications for methodologies to compute sailboat aerodynamics for Velocity Prediction Program design tool.

This paper deals with research activities carried out at Politecnico di Milano Twisted Flow Wind Tunnel in order to investigate the performance of upwind sails in heeled condition. This work is a part of an overall and comprehensive general research program started in 2005 with partial funding from the ORC with the aim to investigate a series of rig planform variations in mainsail roach and jib overlap in order to overcome some perceived inequities in the ratings of boats of various rig design racing under the International Measurement System (IMS).

The results of this investigation are used to assist the International Technical Committee (ITC) in changing the formulations in the ORC INTERNATIONAL VPP sail aerodynamic model.

This paper in the first part presents test arrangements, procedures and methodologies that have been carried out both for systematic gathering of wind tunnel data and subsequent analysis in order to describe aerodynamic behaviour of different sailplans both in upright and heeled condition. Some interesting experimental results and trends are presented and discussed.

Differences of sail performance at different heel configurations outlined by means of wind tunnel test results are clarified with the aid of numerical results obtained using RANS methods performed on the tested sailplan configurations. For this reason, during the tests authors gave special attention to measure also sails flying shapes in order to provide sails geometry useful for CFD purposes.

Paper presents also a detailed description of methods and techniques used by the authors in order to detect sails shapes.

Finally the so called “heeled plane approach” [3], [6], [7] which is largely used in the aerodynamic models

available up to-date for VPP use is outlined and discussed.

## 2. TWISTED FLOW WIND TUNNEL

With the purpose of supporting, with a state of the art facility, the world-wide recognised excellence of Politecnico di Milano research in the field Wind Engineering as well as general Aerodynamics, Politecnico di Milano decided to design and build a new large wind tunnel having a very wide spectrum of applications and very high standards of flow quality and testing facilities. The Wind Tunnel has been fully operative since September 2001 and from the first year of operations has been booked for sailing yacht design applications.

Figure 1 shows an overview of the P.d.M. facility: it's a closed circuit facility in a vertical arrangement having two test sections, a 4 x 4m high speed low turbulence and a 14 x 4m low speed boundary layer test section.

A peculiarity of the facility is the presence of two test sections of very different characteristics, offering a very wide spectrum of flow conditions, from very low turbulence and high speed in the contracted 4 x 4m section ( $I_u < 0.15\%$ ,  $V_{max} = 55 \text{ m/s}$ ), to earth boundary layer simulation in the large wind engineering test section.

With reference to yacht sails aerodynamic studies, they are performed in the boundary layer test section which allows for testing large scale models (typically 1:10 -1:12 for IACC yacht model) with low blockage effects at maximum speed of 15 m/s.

A very important peculiarity concerning yacht aerodynamics is that since the wind speed increases with height due to the boundary layer phenomena and the boat speed is constant, this means that the apparent wind speed incident onto a yacht also increases with height and, in addition, its direction changes, rotating away from the yacht's heading with increased height.

This is a very important topic in wind tunnel testing on sailing yacht scale models, that has to be carefully considered, because the forces developed by the sail plan are due to the apparent wind incident onto the sails and

the sail shape and trim is strongly related to the apparent wind profile.

Therefore, for proper similitude modelling, the apparent wind velocity shear and twist profile has to be reproduced in the wind tunnel for testing stationary models.

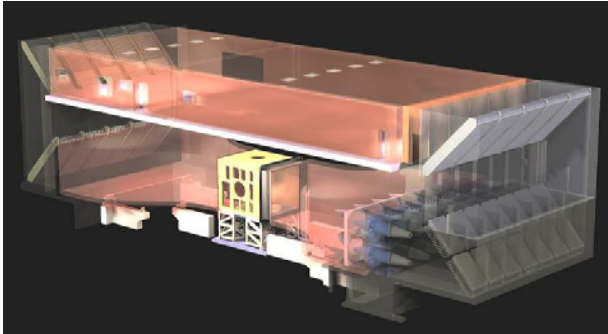


**Figure 1. Politecnico di Milano Wind Tunnel**

While the variation in wind speed with height can be modelled in the wind tunnel using similar procedures as for conventional wind engineering testing, the twisted flow is a more difficult task to deal with for a stationary wind tunnel yacht model, because the true and apparent wind speeds are coincident.

At this purpose the so called Twisted Vanes Device has been designed: the basic idea of the design process is to generate a large-scale vortex with its spin axis aligned with the wind tunnel steady state flow direction, resulting in a twisted flow area corresponding to the model location.

Moreover, basic design requests were the following:

- easy to adjust
- easy to install/remove
- economical solution both in terms of first installation and running costs

The originality of the Politecnico di Milano Twisted Flow Device compared to the other solutions [4] is the central positioning of the device, not occupying the entire tunnel section. In fact, the role of the Twisted Flow Device is just to turn left the lower part and to turn right the upper part of the flow. The side flow not passing through the vanes is allowed to move vertically balancing the flow rate.

Fig. 2 shows the Twisted Flow Device in the tunnel boundary test section.

A complete model, consisting of yacht hull body (above the waterline) with deck, mast, rigging and sails is mounted on a six component balance, which is fitted on the turntable of the wind tunnel (fig. 5). The turntable is automatically operated from the control room enabling a 360° range of headings.

### 3.1 Test arrangements and measurements setup

The large size of the low speed test section enables yacht models of quite large size to be used, so that the sails are large enough to be made using normal sail making

techniques, the model can be rigged using standard model yacht fittings and small dinghy fittings without any additional work becoming too small to handle, commercially available model yacht sheet winches can be used and, most important, deck layout can be reproduced around the sheet winch, allowing all the sails to be trimmed as in real life.



**Figure 2. Twisted Flow Devices**

Moreover the model yacht drum type sheets are operated through a 7 channel proportional radio control system, except that the aerial is replaced by a hard wire link and the usual joystick transmitter is replaced by a console with a 7 multi-turn control knobs that allow winch drum positions to be recorded and re-established if necessary. The sheet trims are controlled by the sail trimmer who operates from the wind tunnel control room.

Figs. 3 show a typical model mounted in the wind tunnel.



**Figure 3. Yacht model in the boundary layer test section**

A high performance strain gage dynamic conditioning system is used for balance signal conditioning purposes. The balance is placed inside the yacht hull in such a way that X axis is always aligned with the yacht longitudinal axis while the model can be heeled with respect to the balance.

The wind tunnel is operated at a constant speed after the wind speed profile and wind twist have been properly tuned considering the desired targets, which are previously calculated considering the potential boat performance at different true wind speeds and yacht courses. As previously said the velocity profile can be simulated by means of independent control of the rotation speed of each fan joined to the traditional spires & roughness technique, while the twist can be simulated by twisting the flexible vanes by different amounts over

the height range. The wind tunnel speed is most usually limited by the strength of the model mast and rigging and the power of the sheet winches.

Data acquisition can be performed in several ways: the usual procedure provides direct digital data acquisition by means of National Instruments Data Acquisition Boards (from 12 to 16 bits, from 8 differential channels up to 64 single-ended) and suitably written programs according to Matlab standards.

The data acquisition software calculates the forces and moments using the dynamometer calibration matrix. The forces are shown in the virtual panel designed on the computer screen in real time so that the sail trim can be optimised because the effects of trimming the sails on the driving and heeling forces can be directly appreciated.

The model is set at an apparent wind angle and at a fixed heel. After a sail trim has been explored, actual measurements are obtained by sampling the data over a period specified by the test manager (generally 30 seconds) with a sample frequency specified too. An important feature of wind testing procedure is that the model should be easily visible during the tests so that the sail tell-tales can be seen by the sail trimmer. For this purposes some cameras placed in the wind tunnel as well as onboard allow a view similar to the real life situation (fig.4).

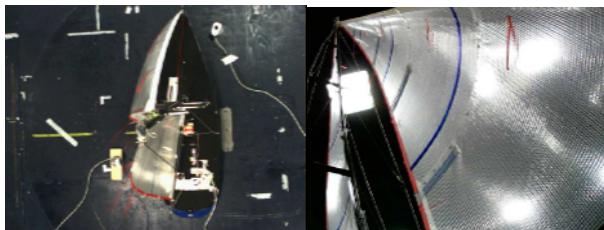


**Figure 4. Wind tunnel top and deck camera view during testing**

In order to correlate force measurement readings and the sail shape and in order to provide input data for CFD calculations, an in-house photogrammetric measuring system has been developed to recover flying shapes during tests (fig.5).

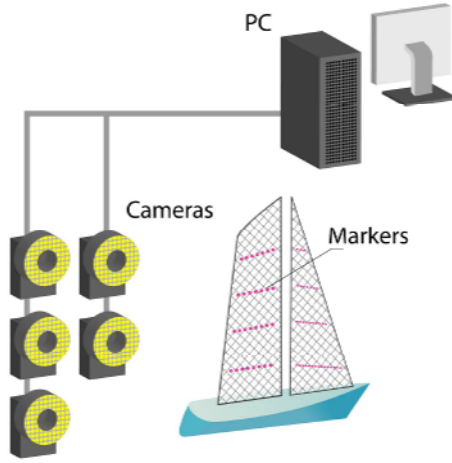


**Figure 5. Flying shape measurement system layout**

The photogrammetry based technique is relatively fast during the tunnel occupancy phase and in principle it requires only three digital images be recorded from useful points. In order to overcome difficulties arising from sails overlapping especially in downwind configurations and in order to be able to have at least three useful points in each part of the sails the system is equipped with eight cameras. For the present tests this system is composed of five cameras, filming reflective targets placed on sails in sync, and a PC equipped with acquiring and processing custom-made software. Cameras have resolution of 1392 x 1040 pixels, greyscale 1/2" CCD sensor, 17 fps (frames per second). Each of them mounts an optical zoom and a high intensity infrared (830 nm) LED illuminator, triggered to simultaneously flash with cameras frame rate. In order to reduce at the best cameras vibrations induced by the wind, it was decided to fix cameras on photographic heads constrained to the available stiffest points in the wind tunnel (fig.6).



**Figure 6. Yacht model and cameras in the wind tunnel**

High reflective markers are glued on 8 horizontal sections of each sail plus one on the top, on both windward and leeward side (fig 7).

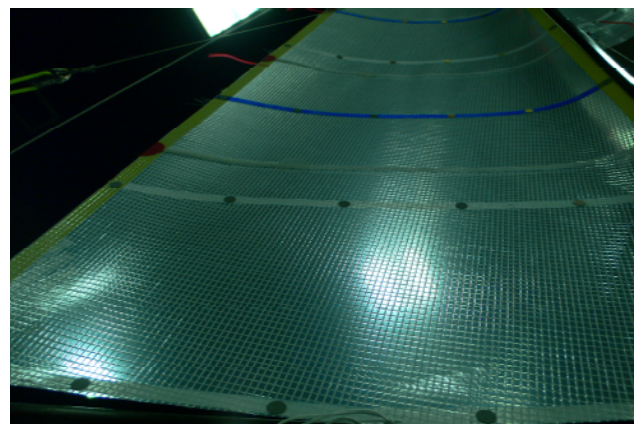


**Figure 7. Reflective markers on the main**

Then, a custom-made software performs real time blob detection and stores images sourced from cameras on a hard disk.

As a result of this routine a table with the 2D blob detected coordinates is available for post process.

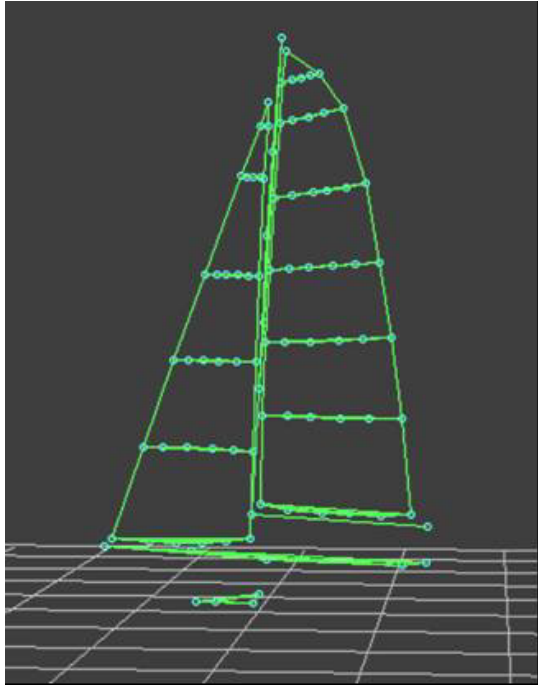


**Figure 8. Sails flying shape detection process**

Cameras have been previously calibrated using a custom built calibration frame.

The 3D marker points coordinate for each sail are then obtained by means of a DLT (Direct Linear Transformation) algorithm, reaching marker position with an uncertainty equal to 0,5 mm.

Marker coordinates are obtained as mean of their position over a 20[sec] acquisition period with 17 Hz acquisition rate.

Then this 3D points array are used for surface modelling as well as to extract the trim parameters as explained in [5].

### 3.2 Upwind sails testing procedure

For each apparent wind angle tested the first task was to reach the maximum driving force potentially achievable. At the same time it was observed the influence of the sails trimming changes using the data acquisition program that visualizes the forces acting on yacht model in real time.

Trimming the sails to obtain optimum sailing points proved to be the most challenging task of the testing process.

Attempts were made to carry out the job as systematically as possible. Firstly, the maximum drive point was found by trimming the sails to the best using the cameras views, the tufts on the sails and the force measurements output data.

From there, the heeling force would be reduced to simulate the trim of the sails for windier conditions. In fact in real life windy conditions, to keep the optimum

heeling angle, heeling force has to be reduced by the crew. The sail trimming routine adopted was to choose the mainsail traveller position (initially quite high up to windward) and then to vary the incidence and the twist of the mainsail to power or de-power it, by over-trimming or easing the main traveller and main sheet.

The genoa was initially trimmed in order to have the maximum driving force condition and was fixed varying the mainsail shape.

Once a specific trimming condition is obtained using the real time force and moments values displayed by the data acquisition system, a 30 seconds acquisition sampling has been performed with 100Hz sample frequency, and both time histories and mean values of each measured quantity have been stored in a file.

The usual way of analysing data is to compare non dimensional coefficients, allowing to compare the efficiency of sails of different total area at different conditions of dynamic pressure. The first analysis performed is the variation of driving force coefficient  $C_x$  with heeling force coefficient  $C_y$ . They are given by the expressions:

$$C_x = \frac{F_x}{\frac{1}{2} \rho S v^2}$$

$$C_y = \frac{F_y}{\frac{1}{2} \rho S v^2} \quad (1)$$

where

- $F_x$  is the driving force
- $F_y$  is the heeling force
- $S$  is the actual sail area
- $V$  is the wind speed
- $\rho$  is air density

As an example fig. 9 shows a comparative plot of  $C_x$  versus  $C_y$  for the apparent wind angles tested. Each run (with its corresponding measured values) is shown for each AWA.

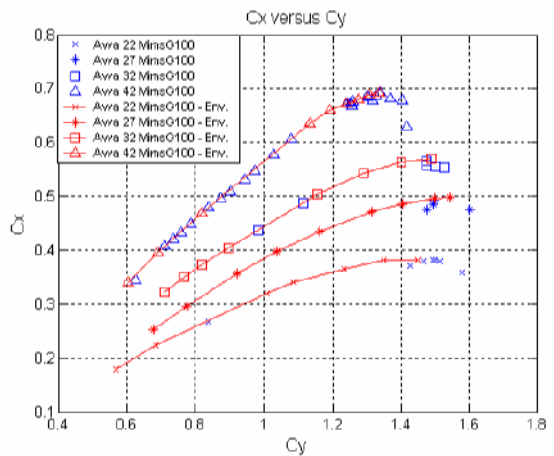


**Figure 9:Driving force coefficient vs heeling force coefficient**

It can be seen that there are some sail settings at the highest values of heeling force coefficients where the driving force is lower than the maximum value. These non optimum values were obtained by oversheeting the

sails such that the mainsail generally had a tight leech and the airflow separated in the head of the sail. Therefore a selection was made to choose those points that formed the envelope curves (maximum  $C_x$  for a given  $C_y$  value) for each apparent wind angle (fig. 9). Envelope curves have been drawn through the test points with the greatest driving force at a given heeling force. An example is reported in fig. 10.

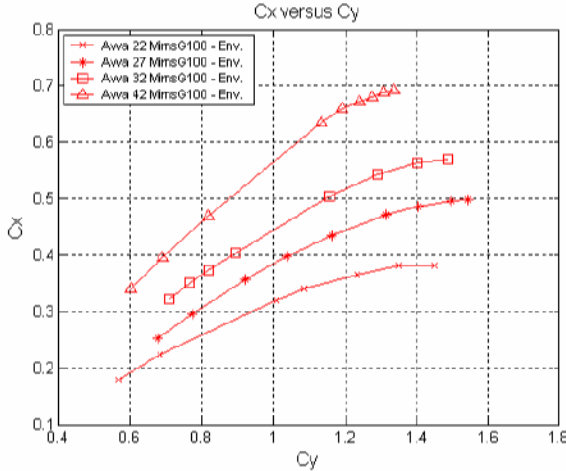


**Figure 10. Driving force coefficient envelope vs heeling force coefficient**

For the purpose of the analysis, in the following only these points will be used.

The centre of effort height,  $C_{eh}$ , is obtained by dividing the roll moment by the heeling force component in the yacht body reference system:

$$C_{eh} = \frac{M_x}{F_y}$$

As an example, a plot of its variation with heeling force for all angles can be seen in fig 11. Both all the measured values and the envelope of the points corresponding to maximum driving force at each heeling force are reported. The results are given in terms of ratio between centre of effort height from boat deck and mast height (P+BAS). The centre of effort longitudinal position,  $C_{ea}$ , is obtained by dividing the yaw moment by the heeling force component in the yacht body reference system:

$$C_{ea} = \frac{M_z}{F_y}$$

As an example, a plot of its variation with heeling force for all angles can be seen in fig 12. Both all the measured values and the envelope of the points corresponding to maximum driving force at each heeling force are reported.  $C_{ea}$  is measured from the origin of the balance (positive to bow) which is placed behind the mast.

The results are given in terms of ratio between centre of effort longitudinal position from balance origin and yacht model waterline length.

It can be seen that  $C_{ea}$  moves forward as  $C_y$  reduces. This is explained by the way the sails are de-powered.

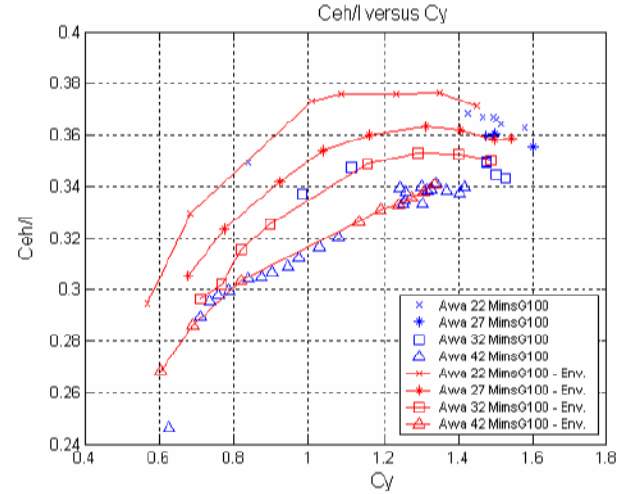


**Figure 11. Centre of effort height vs heeling force coefficient**

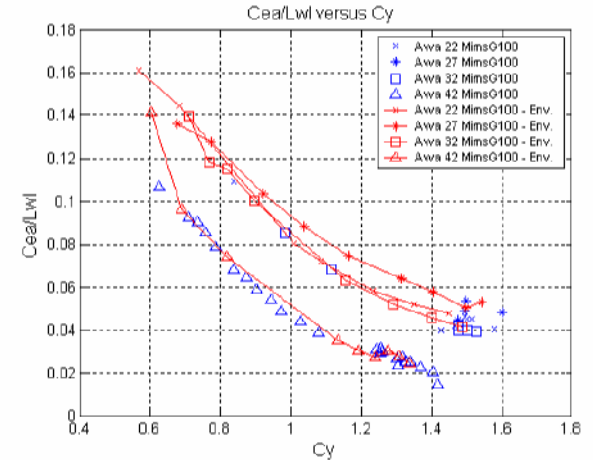


**Figure 12. Centre of effort longitudinal position vs heeling force coefficient**

### 3. SAILPLANS TESTED

According to the overall activities program 3 different main sails (with the same actual area but 3 different roaches) named Mims, Mhr, and Mtri and 3 different jibs with different overlap (named G100, G135 and G150) have been combined in a 92% fractionality configuration.. Note that the Mims mainsail has the IMS maximum allowed roach without any penalty applied according to the IMS rule.

Mainsail Roach level has been defined according to:

$$Roach = \frac{Area_{Main}^{IMS}}{P * E / 2} - 1 \quad (2)$$

Mainsails codes and dimensions are defined as follows:

	Roach	P	E
Mims	0.193	1.94	0.637
Mhr	0.335	1.94	0.571
Mtri	0.096	1.94	0.695

**Tab. 1**

Jib codes are defined as follows:

	Overlap
G100	100%
G135	135%
G150	150%

**Tab. 2**

All configurations were tested in upright condition and at 30° heeling too.

Only the IMS mainsail+135% jib have been tested at 15° heeled condition too.

Table 3 summarises the situation.

	Upright	Heel 15°	Heel 30°
Mims G100	X		X
Mims G135	X	X	X
Mims G150	X		X
Mhr G100	X		X
Mtri G100	X		X

**Tab. 3**

Figures 13-17 show the different sailplans during the tests.



**Figure 13. MhrG100 sailplan**



**Figure 14. MtriG100 sailplan**



**Figure 15. MimsG100 sailplan**

Apparent wind angles were chosen to be 22°, 27°, 32° and 42° which cover the upwind range.

For each apparent wind angle, sail trimming during the wind tunnel tests were performed according to the abovementioned procedure. All the sails trimming have been performed by Gigio Russo of North Sails Italia using the remote control console for model winches. At the same time it was observed the influence of the sails trimming changes using the data acquisition program that visualizes the forces acting on yacht model in real time.



Figure 16. MimsG150 sailplan



Figure 17. MimsG135 sailplan

#### 4. EXPERIMENTAL RESULTS

Using the aerodynamic driving force and aerodynamic heeling moment  $F_x$  and  $C_{Mx}$  component in the yacht body reference system the corresponding coefficients have been obtained as follows:

$$C_x = \frac{F_x}{\frac{1}{2} \rho S V_a^2} \quad (3)$$

$$C_{Mx} = \frac{M_x}{\frac{1}{2} \rho S H_{mast} V_a^2}$$

where

- $F_x$  is the driving force

- $M_x$  is the heeling moment
- $S$  is the actual sail area
- $H_{mast}$  is the mast height from the deck
- $V_a$  is apparent wind speed
- $\rho$  is air density

The apparent wind speed  $V_a$  and apparent wind angle are evaluated in the heeled plane perpendicular to the mast according to:

$$V_a = \sqrt{(-V_t \cos \gamma)^2 + (V_t \sin \gamma \cos \phi)^2} \quad (4)$$

$$AWA = \arctg \left( \frac{V_t \sin \gamma \cos \phi}{-V_t \cos \gamma} \right)$$

where  $\gamma$  represent the true wind angle (yaw angle),  $V_t$  is the wind tunnel flow velocity corresponding to the mean dynamic pressure at each run and  $\phi$  is the heel angle.

Figures 18-21 show test results relevant to the mainsail medium roach and medium overlapping jib (MimsG135) sailplan in terms of envelope curves (maximum  $C_x$  for a given  $C_{Mx}$  value) for each apparent wind angle.

In particular in each figure results are reported with reference to each apparent wind angle tested in upright and heeled condition too: in this case the resulting apparent wind angle according to eqn. 4 is shown in the legend.

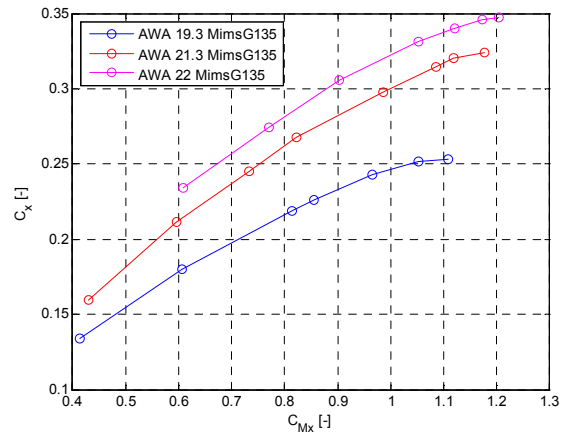


Figure 18. MimsG135 sailplan

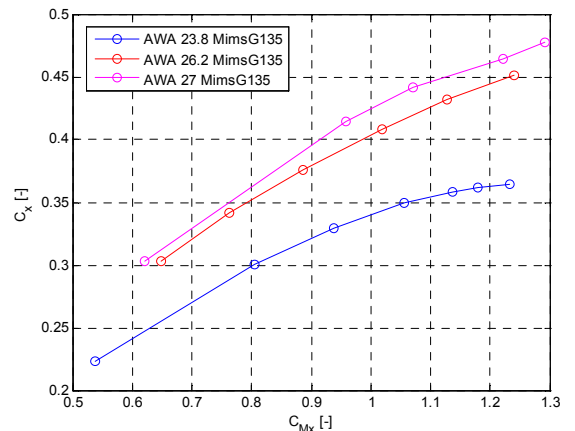


Figure 19. MimsG135 sailplan

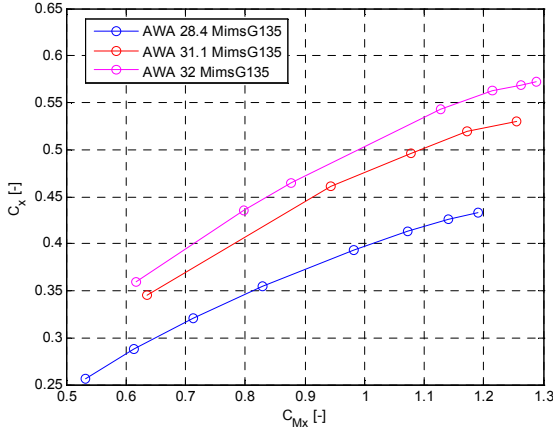


Figure 20. MimsG135 sailplan

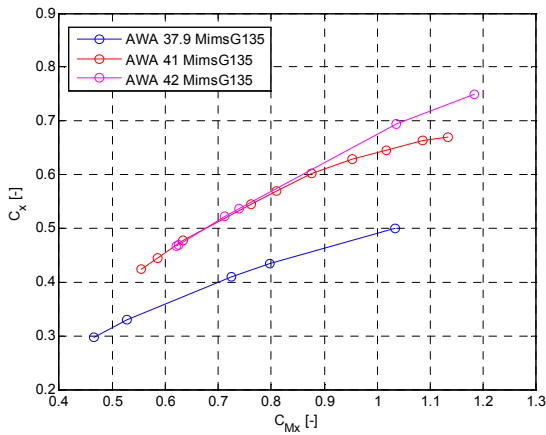


Figure 21. MimsG135 sailplan

As can be seen the effect of heel is to reduce the maximum driving force produced by sails at each apparent wind angle tested and this effect increases with the heeling angle increasing.

The same situation has been found for each sailplan tested: as an example figures 22-25 refer to max roach mainsail with non overlapping jib (MhrG100).

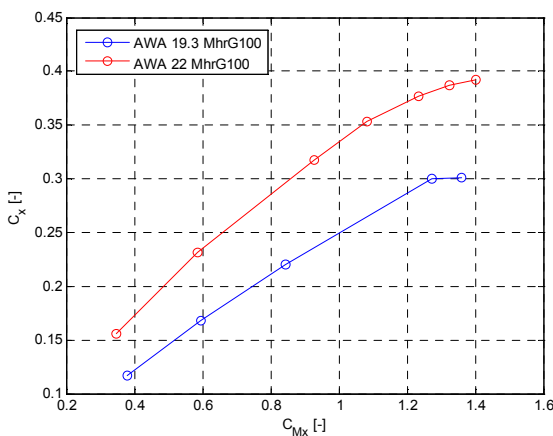


Figure 22. MhrG100 sailplan

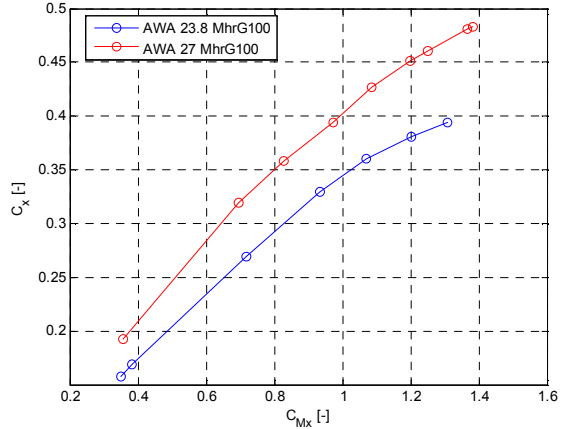


Figure 23. MhrG100 sailplan

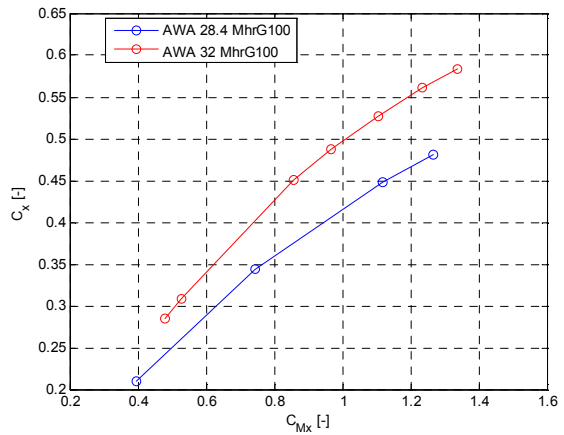


Figure 24. MhrG100 sailplan

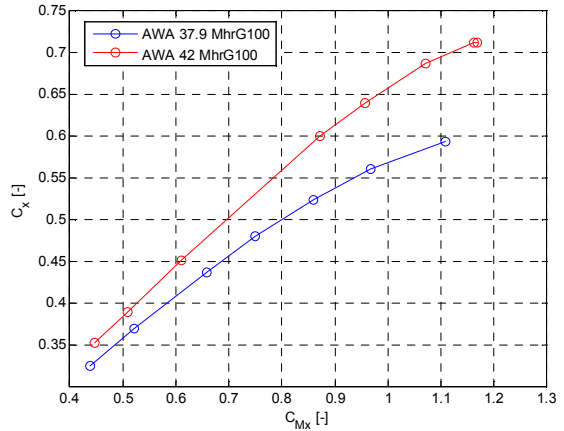
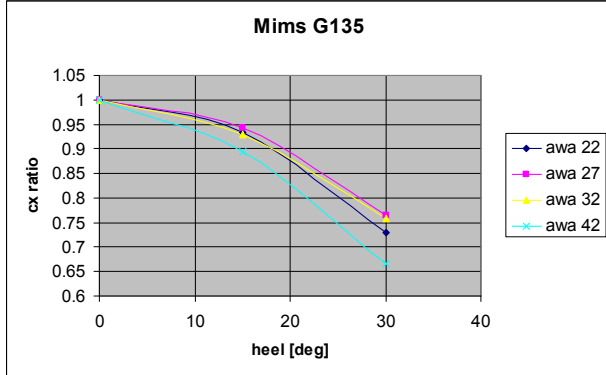


Figure 25. MhrG100 sailplan

Another interesting feature is that the reduction in driving force is more evident in fully powered condition than in the depowered ones and this is a general trend for each sailplan tested.

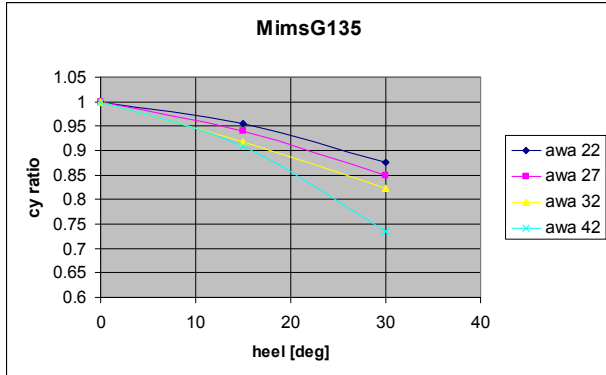
With reference to the mainsail medium roach and medium overlapping jib (MimsG135) sailplan figure 26 shows the ratio between the driving force coefficient at different heel angle and the same quantity in upright condition for each apparent wind angle relevant to the

sailplan trim allowing for the maximum driving force. These ratio can be interpreted as a sort of efficiency parameter of the sailplan heeled condition.



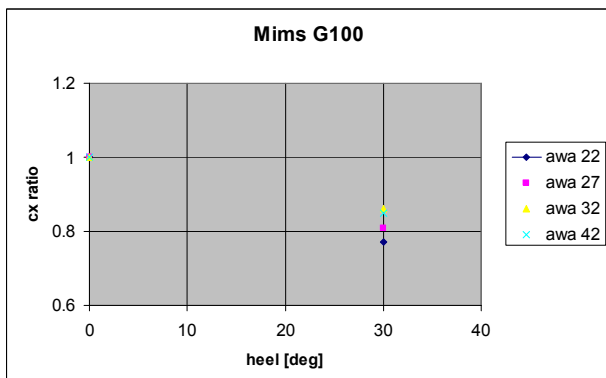
**Figure 26. MimsG135 sailplan**

Figure 27 is relevant to heeling force coefficient ratio of the same (MimsG135) sailplan.



**Figure 27. MimsG135 sailplan**

All the performed tests revealed a decrease in sailplan driving force when the sailplan heels (figures 28-31).



**Figure 28. MimsG100 sailplan**

In order to gain further understanding of the sailplans aerodynamic behaviour experimentally outlined numerical simulations have been carried out using RANS methods. In particular numerical simulations have been performed by means of FLUENT CFD code with the realizable k- $\epsilon$  turbulence model. A numerical model of each tested sailplan including hull and rigging has been

carried out and put in the numerical model of the wind tunnel (figure 32). The boundary conditions were set to give a wind velocity profile similar to that in the wind tunnel.

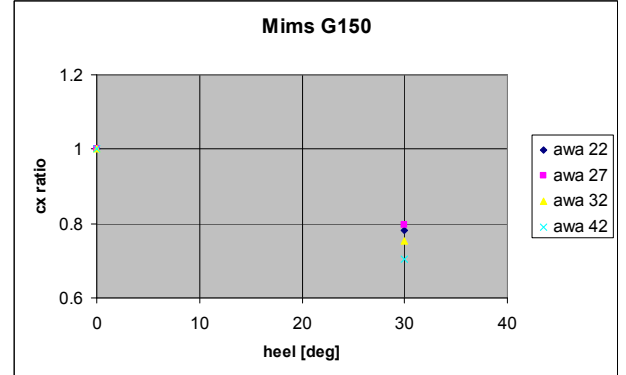


**Figure 29. MimsG150 sailplan**

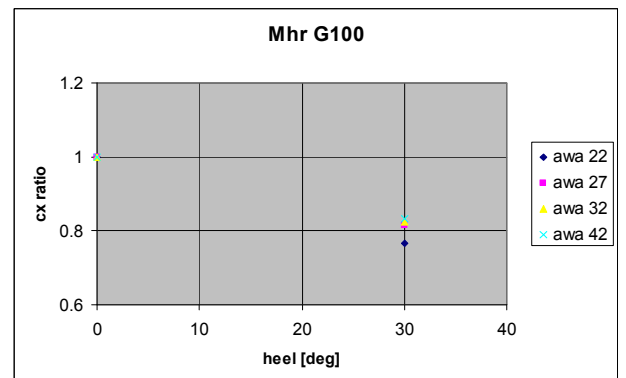


**Figure 30. MhrG100 sailplan**

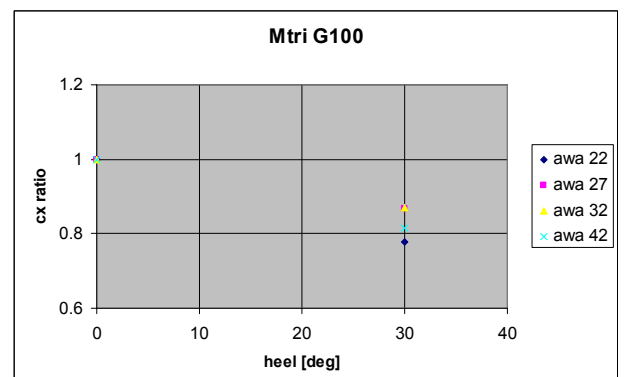


**Figure 31. MtriG100 sailplan**

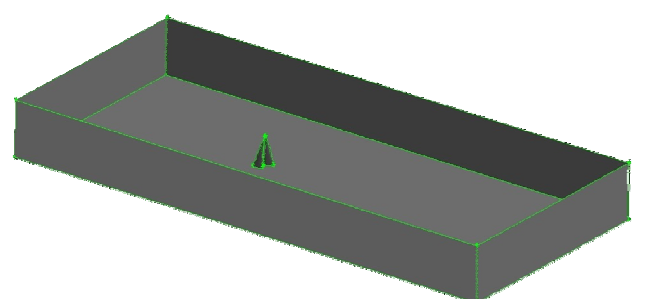


**Figure 32. Wind tunnel and yacht numerical model**

In the following, for lack of space, results concerning only the medium roach mainsail with non overlapping jib (MimsG100) will be reported.

Fig. 33 shows numerical model of sails including yacht hull, which has been used to simulate yacht upwind behaviour at different heel angles (sailing upright, 15°heeled and 30° heeled).

Numerical simulation have been performed at 22° apparent wind angle and for each of the heel angle considered the flying shape corresponding to maximum drive condition trimming at different heel angle has been used in order to generate the numerical mesh.

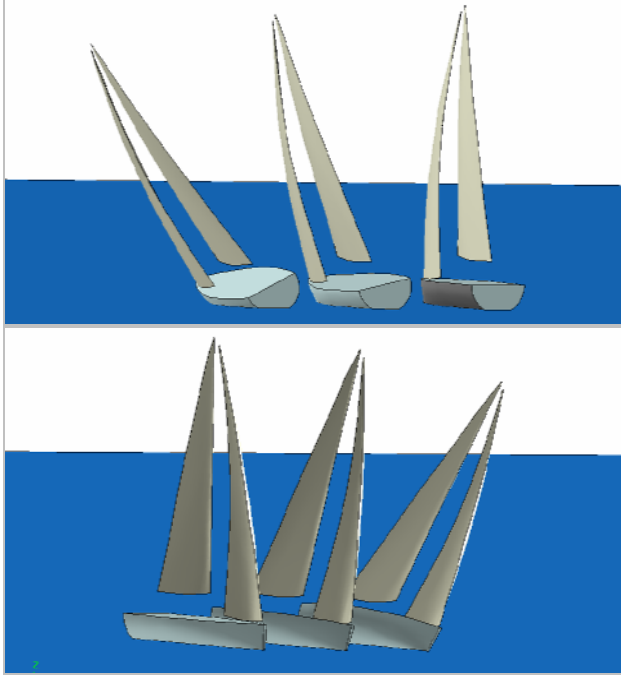


**Figure 33. MimsG100 sailplan numerical model**

Figures 34-35-36 show the MimsG100 sailplan leeward side pressure coefficient contour respectively for upright, 15°heeled and 30° heeled condition concerning 22° apparent wind angle close hauled sailing condition analysis.

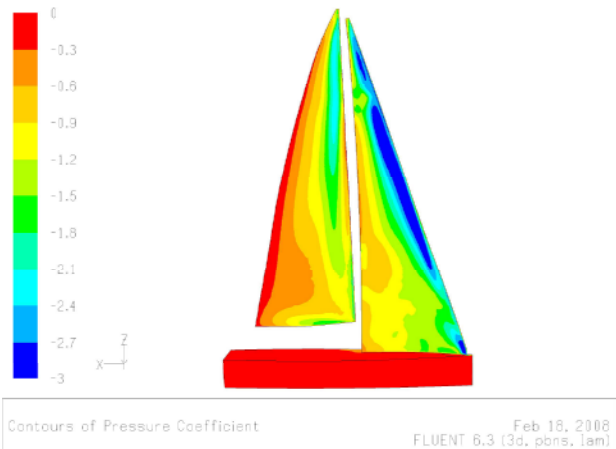


**Figure 31. Leeward Cp contours in upright condition**

As can be seen heel increasing result in a less of a pressure drop on both the sails, due to pressure decrease

on the sailplan windward side; moreover in the lower part of the jib pressure increases with heel reducing the suction on the leeward side.

In order to understand this behaviour it's useful to refer to figures 41-42 which show the flow velocity vectors coloured by magnitude (normalised to the free stream incoming flow) in a plane perpendicular to the mast at 25% of mast height from the deck respectively for upright, 15°heeled and 30° heeled conditions.

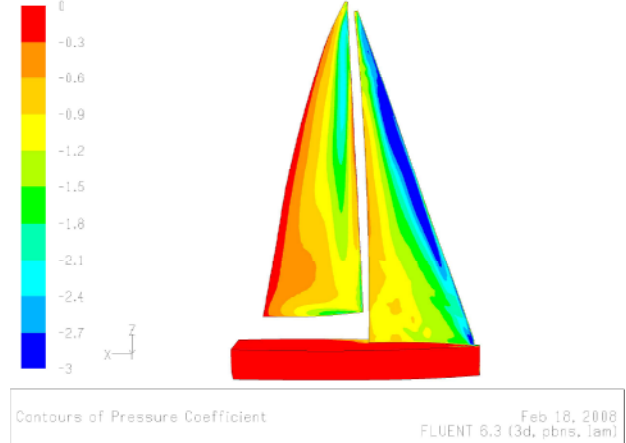


**Figure 35. Leeward Cp contours at 15° heel**

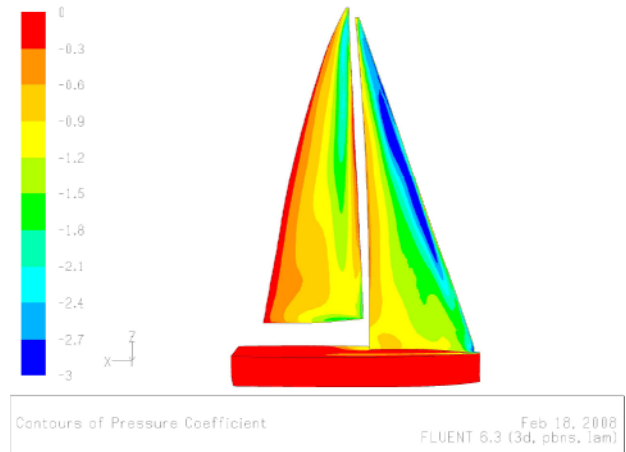


**Figure 36. Leeward Cp contours at 30° heel**

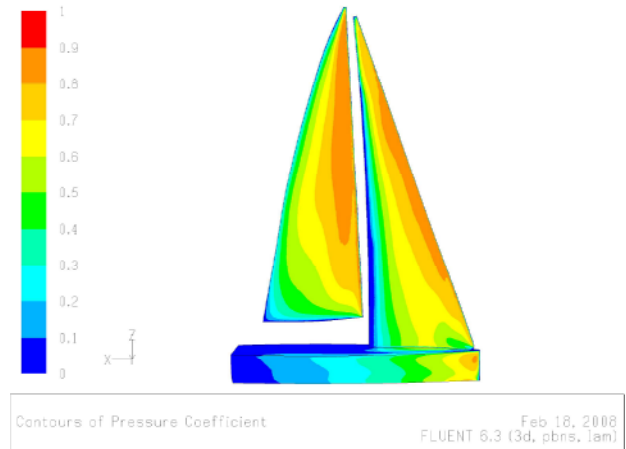


**Figure 37. Windward Cp contours in upright condition**

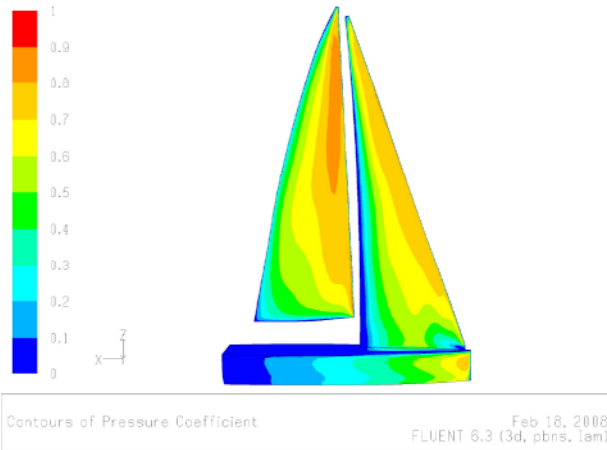


**Figure 38. Windward Cp contours at 15° heel**

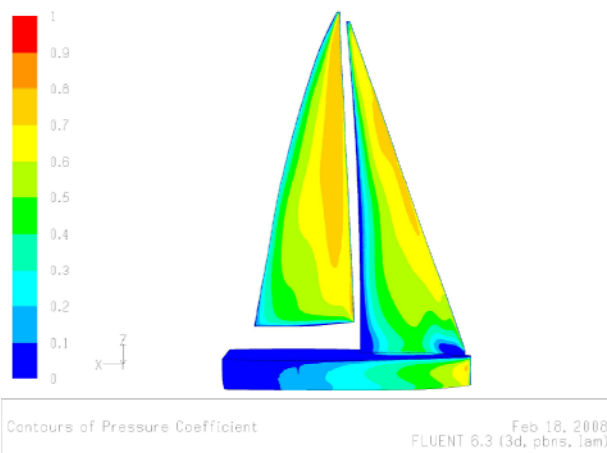


**Figure 39. Windward Cp contours at 30° heel**

When the yacht heels flow angle of attack reduces and the corresponding lift decreases, leading to a reduction of the driving force too. As can be seen upright condition is associated to some separation on the jib leeward side which disappears at higher heel angles, leading to a lift reduction too.

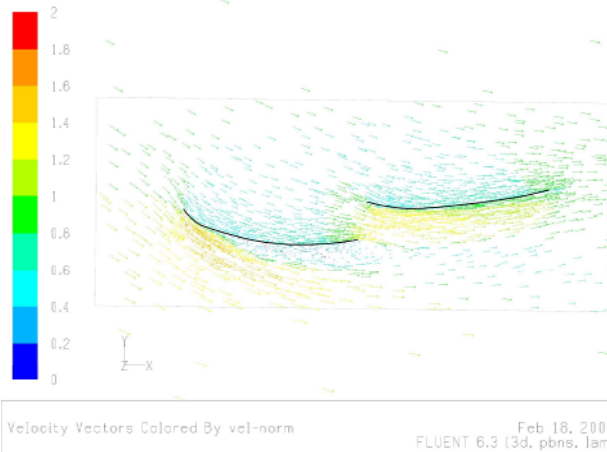


**Figure 40. Velocity vectors in a plane perpendicular to the mast (25% mast height) in upright condition**

This flow behaviour around the sails confirms also the apparent wind angle reduction associated to heeling as

stated by the heeled plane model described in the next paragraph.

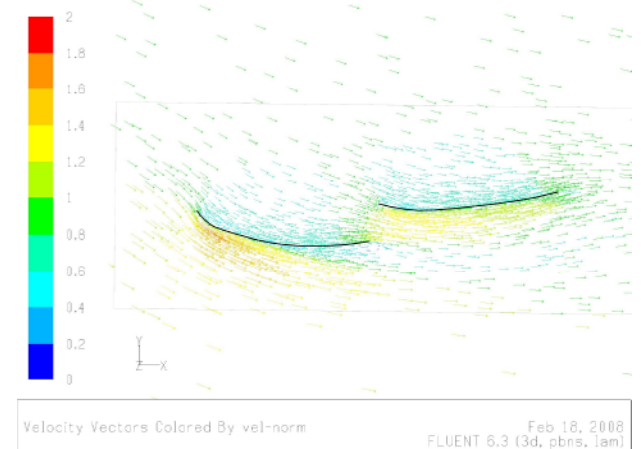


**Figure 41. Velocity vectors in a plane perpendicular to the mast (25% mast height) at 15° heel**

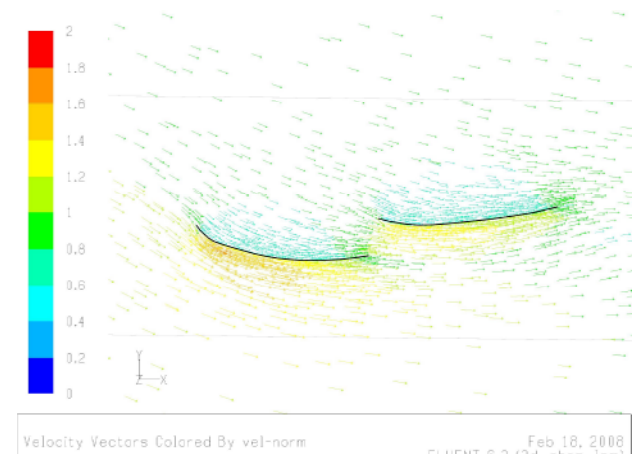


**Figure 42. Velocity vectors in a plane perpendicular to the mast (25% mast height) at 30° heel**

## 5. AERO MODELLING AND HEELED PLANE APPROACH: SOME CONSIDERATIONS

Since 1978 when the first velocity prediction programs for yachts was officially introduced for rating purposes the problem of modelling sail forces is a fundamental focus.

With reference to most of up to date available VPPs it can be said that aerodynamic model is mainly derived from the first aerodynamic model well known as Kerwin model [3].

Many principles of the aerodynamics of sails can be taken from the thin airfoil theory even if significant differences can be found: in a similar way to a wing yacht sails are lifting bodies where due to their shapes and the direction of the onset flow circulation appears increasing fluid velocity on the leeward side and decreasing velocity in the windward side with a

consequent high pressure region on the windward side and low-pressure region on the leeward side.

The lift and drag forces, resulting from the pressure regions around the sails can be expressed in terms of non-dimensional coefficients so that any forces and moments can be evaluated considering actual sail area and dynamic pressure of the free stream onset speed of the flow.

With reference to a wing the lift and drag coefficients are primarily a function of the angle of attack: on a sailing yacht this quantity is not easy to be defined due to continuous sails shape changing due to sails trimming. Hence in case of sails the angle of attack concept is replaced by the apparent wind angle which is the angle between the relative free-stream onset flow and the yacht centreline.

Moreover the free-stream speed of the onset flow to be used in evaluate the dynamic pressure is usually considered to be the apparent wind speed.

Wind tunnel tests and full scale experiments are the most suitable way to evaluate the drag and lift coefficients of the sailplan for different apparent wind angles considering the sails geometry, the relative direction of the onset flow, the flow structure (gradient and twist) and the trim of the sails.

A typical representation of forces acting on the sailplan are based on lift and drag sailplan coefficients plotted against the apparent wind angle.

The effect of heel is generally taken into account using the so called effective angle theory [Jackson, Campbell] which is used to address the fact that the heel angle influences the flow around the sails since the onset flow can always been considered as being horizontal. As the yacht heels the onset flow is not longer perpendicular to the leading edge of the sails and due this the resulting lift and drag forces are different for each heel angle.

Each aero model must take into account for the fact that lift and drag coefficients are no only a function of the apparent wind angle but also of the yacht heel.

Kerwin [3] and the so called effective angle theory assume that the sails are insensitive to the flow component along their span (i.e. along the mast) and that only the flow component perpendicular to the mast produces the lift and drag forces.

This represents one of the tougher issue of upwind aerodynamics and some discussions have been found in literature also very recently [Jackson 2001], [Teeters Sea Horse].

Aim of this paragraph is to discuss the appropriateness of this assumption and to investigate in more details its consequences on results available from aero models based on this underlying hypothesis.

More in details the flow component along the chord of the sails can be seen as the flow component in the heeled plane, which is a plane perpendicular to the mast and this means that the sails are insensitive to the flow component along the mast.

As an example in fig. 44 all tests performed by the authors for MimsG100 sail plan are reported (136 runs).

In particular for each test performed (as indicated on the abscissa axis named “prove” in fig. 44) the 3 component of the aerodynamic measured force are reported.

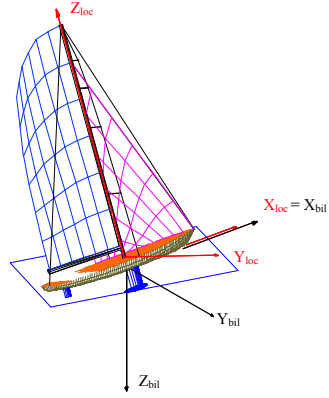


**Figure 43. Balance and boat reference systems**

With reference to fig. 44 blue symbols are relevant to balance axes aerodynamic force components (named “bil”) while red symbols are relevant to the boat reference system values (named “loc”) defined in fig. 43. More in details in figure 44:

- Runs 1-16 are 22° AWA and 30° heel tests
- Runs 17-28 are 27° AWA and 30° heel tests
- Runs 29-42 are 32° AWA and 30° heel tests
- Runs 43-62 are 22° AWA and 30° heel tests
- Runs 63-95 are 42° AWA and upright tests
- Runs 96-109 are 32° AWA and upright tests
- Runs 110-122 are 27° AWA and upright tests
- Runs 123-136 are 22° AWA and upright tests

As can be seen the aerodynamic force component along the mast (“zloc” component) is quite zero except for the 42°AWA runs: this was a systematic effects shown by tests with each sailplan tested.

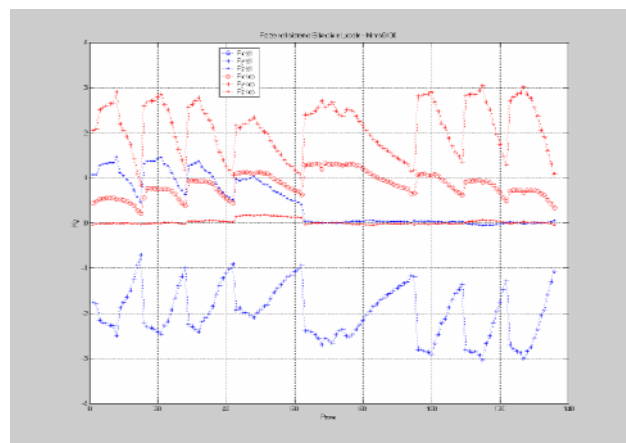


**Figure 44. MimsG100 runs sequence**

Experimental measures demonstrate that Kerwin assumption that the sails are insensitive to the flow component along the mast is substantially verified.

Coming back to the “heeled plane” model, the flow component in the heeled plane is called the effective flow and is defined by the effective angle and effective speed according to the following equations:

$$V_a = \sqrt{(-V_t \cos \gamma)^2 + (V_t \sin \gamma \cos \phi)^2} \quad (5)$$

$$AWA = \arctg \left( \frac{V_t \sin \gamma \cos \phi}{-V_t \cos \gamma} \right)$$

where  $\gamma$  represent the true wind angle (yaw angle),  $V_t$  is the true wind speed and  $\phi$  is the heel angle.

Using the driving and heeling aerodynamic force  $F_x$  and  $F_y$  component in the yacht body reference system the corresponding drag and lift forces components can be obtained as follows:

$$DRAG = -F_x \cos(AWA) + F_y \sin(AWA) \quad (6)$$

$$LIFT = F_x \sin(AWA) + F_y \cos(AWA)$$

Then the corresponding drag and lift coefficients  $C_D$  and  $C_L$  can be evaluated:

$$DRAG = \frac{1}{2} \rho V_a^2 C_D(AWA) S \quad (7)$$

$$LIFT = \frac{1}{2} \rho V_a^2 C_L(AWA) S$$

where  $S$  is the actual sailplan area.

So when the boat heels over the apparent wind angle decreases and the apparent wind speed reduces and this results in a loss of aerodynamic drive force.

This approach is very interesting because only one set of sails coefficients can be used to any heel angle.

As an example in figures 45-46 the  $C_D$  and  $C_L$  measured values at different AWA are reported for the medium roach mainsail+ non overlapping jib in upright condition. At each AWA, values corresponding to each run (i.e. each trim) performed are reported and red full dots correspond to the maximum driving force condition trimming point.

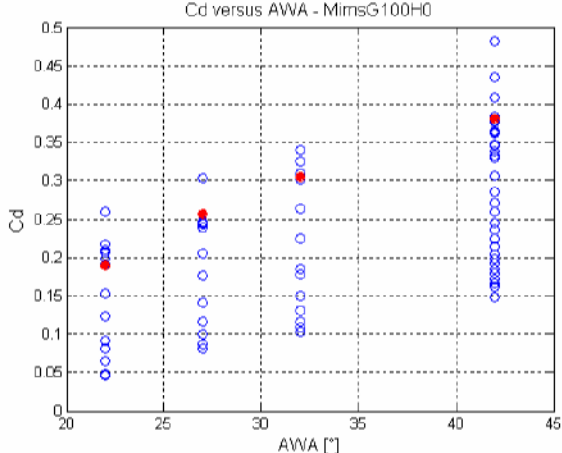


Figure 45. Drag coefficient vs apparent wind angle

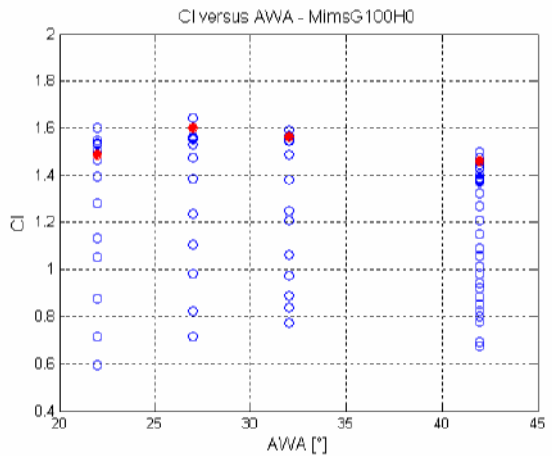


Figure 46. Lift coefficient vs apparent wind angle

Heel effect on sails aerodynamics is outlined in the following: in figures 43-44 the measured  $C_D$  and  $C_L$  values defined using the effective wind angle and effective wind speed according to eq.(5) are reported for the 30° heel condition too.

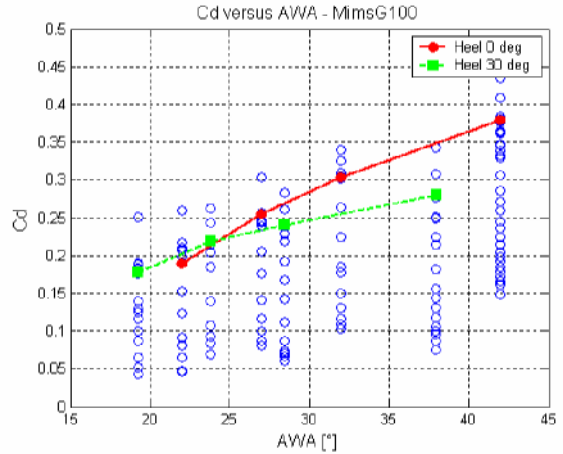


Figure 47. MimsG100 drag coefficient

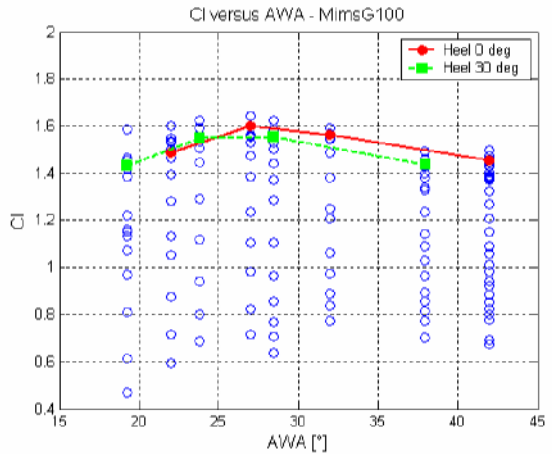


Figure 48. MimsG100 lift coefficient

Figures 49-50 refer to the medium roach + medium overlapping sailplan where upright, 15° heel and 30° heel configuration are reported.

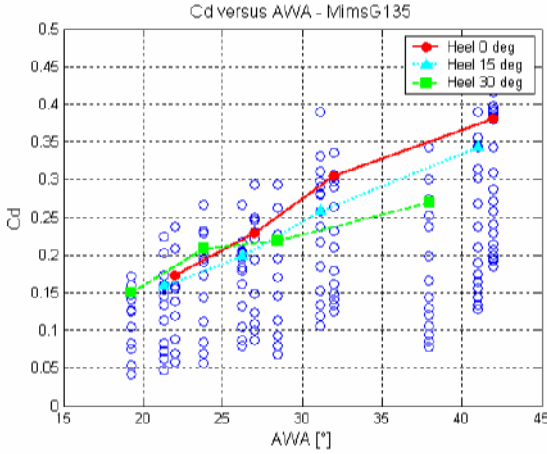


Figure 49. MimsG135 drag coefficient

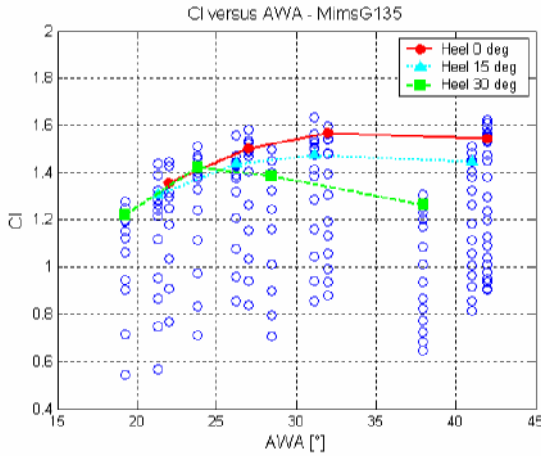


Figure 50. MimsG135 lift coefficient

As a general comment from the experimental obtained result it can be seen that  $C_D$  and  $C_L$  curves tend to be different with respect to AWA at different heels and differences are larger at wider apparent wind angles. This trend is confirmed also for all the other sailplan tested (not reported here for lack of space reasons).

It should be also noticed that using the so called effective angle approach implies to move to any heel angle on the upright condition coefficients curves, depending on the effective wind angle, leading to a general lift and drag overestimation at wider angles while at the closer angles this error is going to reduce.

The corresponding situation for the abovementioned sailplan in terms of drive and heeling force is outlined in figures 51-52.

As can be seen at wider apparent wind angle using upright condition coefficients and effective wind angle both forces are overestimated.

This could also explain the reason why VPP solutions are generally obtained in association with large values of flat parameter: in fact depowering introduced by flat values sometime less than 0.5-0.6 are not realistic and probably due to overestimation of aerodynamic forces in heeled conditions.

An approach more consistent with experimental data could be to use  $C_D$  and  $C_L$  values, depending on actual

yacht heel and on the actual apparent wind angle, obtained from an interpolation between the available experimental database.

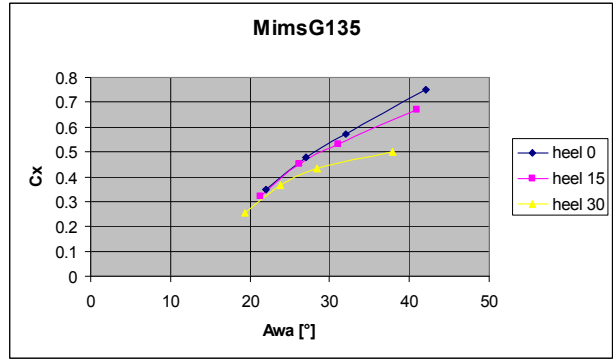


Figure 51. MimsG135 driving force coefficient

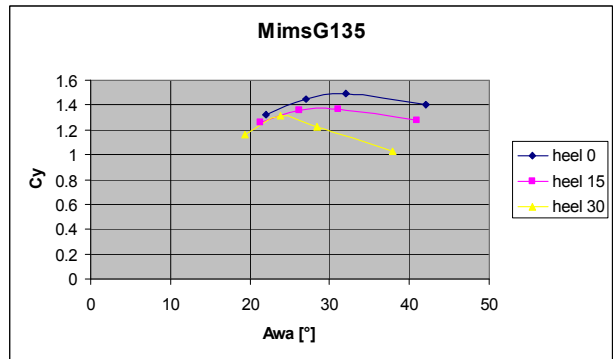
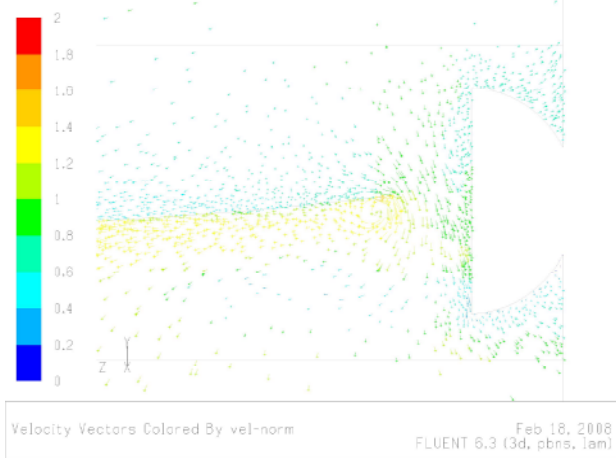


Figure 52. MimsG135 heeling force coefficient

Finally it's also interesting to mention that results and conclusion of the present paper go exactly in the opposite direction with respect of results presented in [8]. Despite that only qualitative results are reported in that paper without any details on the sailplan tested available, it's author's opinion that in principle results showing that there is no drop-off in driving force over the entire operational range of the sails until 30° heel are not particularly surprising and can be explained considering sails-hull interaction effects. Some wind tunnel tests recently performed by the authors on a IACC Version 5 yacht model on upwind sails at various heel angles (not reported here for confidentiality reasons) reveal that at 20° heel the effect of heel was to produce low base drag compared to other heel and associated higher driving force but that could be attributed to changes in the windage drag with heel: this moreover offers the prospect of investigating this feature together with hull shape to reduce windage at different heel angles.

Another important point outlined from author's performed tests and affecting aerodynamic forces with heel was related to the boom height with respect to the deck: figure 53-54 show the wind velocity vectors coloured by normalisation to the free stream incoming flow in a vertical transverse plane that cuts the mainsail at 33% of boom length (from the mast) respectively for

upright, 15°heeled and 30° heeled conditions obtained from the abovementioned numerical simulations.



**Figure 53. Velocity vectors in a vertical plane perpendicular to the boom in upright condition**

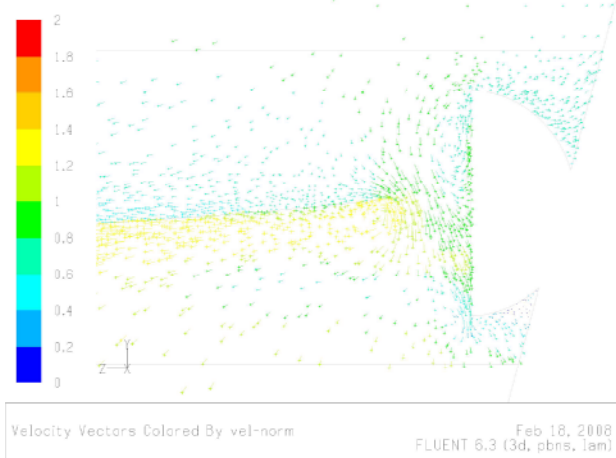


**Figure 54. Velocity vectors in a vertical plane perpendicular to the boom at 15° heel**

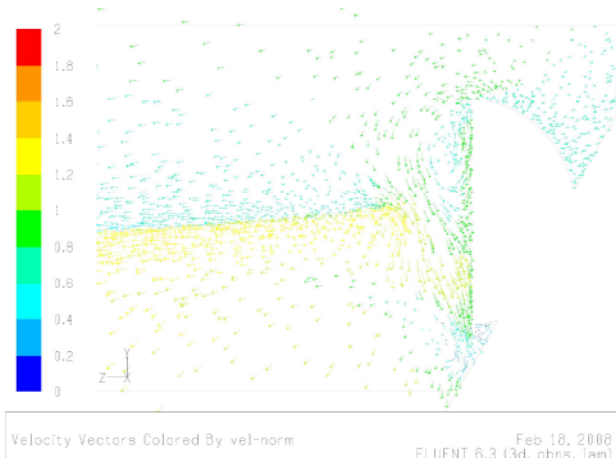


**Figure 55. Velocity vectors in a vertical plane perpendicular to the boom at 30° heel**

These figures show that a vortex generated by deck edge which increases with heel, but that doesn't affect substantially the flow under the boom: this leads to the angle of attack reduction associated to heel increasing the main reason in decreasing sailplan developed forces.

## 6. CONCLUSIONS

This paper gives an overview of the large amount of research activities carried out at Politecnico di Milano Twisted Flow Wind Tunnel in order to investigate the performance of upwind sails in heeled condition. Several rig planform variations in mainsail roach and jib overlap have been tested. Experimental results show that sailplan aerodynamic forces reduce with heeling, that drag and lift coefficients curves are different with respect to apparent wind angle at different heels and differences are larger at wider apparent wind angles.

This trend is confirmed for all the sailplan tested and has been clarified with the aid of numerical results obtained using RANS methods performed on the tested sailplan configurations.

Experimental results reveal that to the so called "heeled plane approach", largely used in the standard VPP aerodynamic models, leads to a general lift and drag overestimation at wider angles while at the closer angles this error is going to reduce. Main conclusion is that with reference to standard applications the so called heeled plane approach is quite adequate even if at upwind wider apparent wind angle both forces are overestimated.

Potential improvement of the generally used Kerwin's assumptions based aerodynamic model, in order to take into account heel effects, are finally outlined based on the available experimental database.

## References

1. J. M. C. Campbell, & A. R. Claughton – Wind Tunnel Testing of Sailing Yacht Rigs – *13<sup>th</sup> HISVA symposium* – Amsterdam 1994
2. Fossati F. et al., ‘Wind Tunnel Techniques for Investigation and Optimization of Sailing Yachts Aerodynamics’, *High Performance Yacht Design Conference Auckland*, 14-16-Feb. 2006
3. Kerwin, JE “A velocity Prediction Program for Ocean racing yachts”, Rep 78-11 MIT, July 1978
4. Fossati, F.& Zasso, A.& Viola I., “Twisted Flow Wind Tunnel Design for Yacht Aerodynamic Studies”, Proc. of the 4th European and African Conference on Wind Engineering, J. Naprstek & C. Fisher, Prague, 11-15 July, 2005.
5. Fossati F. et al, “Experimental Database of Sails Performance and Flying Shapes in Upwind Conditions” Innov’sail 2008, RINA 29-30 May Lorient, 2008
6. P. S. Jackson, “Modelling the Aerodynamics of Upwind Sails” – Journal of Wind Eng. & Ind. Aerodyn., vol. 63 , 1996
7. P. S. Jackson, “An improved Upwind Sail Model for VPPs” – SNAME 15th CSYS, Annapolis, 2001
8. Teeters J., “The Story so Far”, SeaHorse Magazine, July 2007

